Raypath-consistent shear wave statics

Raul Cova*, David Henley and Kris Innanen,
CREWES, University of Calgary, rjcova@ucalgary.ca

Summary

Shear-wave statics are one of the main problems in converted-wave processing. The lack of a good correlation between P- and S-wave velocities in the near surface introduces a whole new problem to be solved. Due to very low velocity values the magnitude of the S-wave statics is several times larger than the P-wave statics, producing a very destructive effect when stacking traces. In this paper it is shown how S-wave statics may also show non-stationary behaviour. This effect was studied in terms of variations in the transmission angle through the low velocity layer (LVL) due to changes in offset and as a result of the structure of the LVL. Although PS-conversions have steeper raypath angles on the receiver side, the presence of dip at the base of the LVL causes a deviation of the rays out of the near-vertical condition. An analytic expression for computing deviated travel times through the LVL in terms of its dip, thickness and velocity is proposed here. This expression may be used as the engine for an iterative non-linear inversion algorithm that will allow us to compute velocity models for the near surface given a set of delay times and the raypath angles associated with them.

Introduction

Conventionally, near surface statics, either for P- or S-waves, are addressed by assuming surface consistency and stationarity in the behaviour of the delay times (Cox, 1999). Henley (2012) explains how these concepts start to fail when the velocity of the near surface is higher than the underlying medium (e.g. permafrost, surface carbonates) or when large lateral changes of velocity may lead to multi-path arrivals. In this work we study the change in static times due to variations of the angle of propagation of the wavefield through the low velocity layer (LVL). By using ray-tracing and finite-difference modelling we show how the near surface statics may become non-stationary. Both the effect of velocities and the geometry of the LVL are addressed in order to achieve an analytical expression for modelling raypath-dependent traveltimes. Although it is not part of this study, this will allow us to develop a new method for computing near surface velocity models by solving raypath-dependent statics.

S-wave static non-Stationarity

Most conventional approaches for statics solution rely on the assumption of nearly-vertical raypaths through the LVL responsible for statics. However, the low velocity of S-waves magnifies the delays in travel time produced by the violation of the vertical-raypath assumption. For a LVL model with 100 m thickness and S-wave velocity V_s =500 m/s, for instance, a deviation of 30º is translated into an extra delay of 30 ms respect to the vertical traveltime. This delay is of the same order of magnitude as P-wave refraction statics. Hence, we need to correct this extra delay to get an optimum stack.

Using Snell's law it is possible to compute the transmission angle of a wavefield propagating through the LVL. As in equation 1, the transmission angle (ϕ_{LVL}), of an upcoming wavefield with incident angle (ϕ_1) depends on the velocity ratio between both media. It is important to note that the LVL interface is assumed to be horizontal and both angles are relative to the normal defined by the interface.

$$\frac{\sin(\phi_1)}{v_1} = \frac{\sin(\phi_{LVL})}{v_{LVL}}. \tag{1}$$

Solving equation 1 for $\sin(\phi_{LVL})$,

$$sin\phi_{LVL} = \frac{v_{LVL}}{v_1}sin\phi_1, \tag{2}$$

Equation 2 can be used for understanding the effect of the velocity contrast on the transmission angle. When $v_{LVL} \ll v_1$, the ratio $v_{LVL}/v_1 \approx 0$, and regardless of the magnitude of the incidence angle ϕ_1 the transmission angle ϕ_{LVL} will be close to zero, i.e. close to the normal to the interface. This is the basic condition which supports the assumption of vertical ray-paths through the LVL. However, when the ratio $v_{LVL}/v_1 \approx 1$, the transmission angle will have a magnitude close to that of the incidence angle. Therefore, we can state that the velocity ratio v_{LVL}/v_1 has the effect of constraining the range of angles in which a wavefield may be transmitted. This supports the idea that if the velocity contrast between the near surface and the medium beneath is smooth, large transmission angles in the LVL can be reached leading to raypath-dependent statics.

One additional degree of complexity can be introduced if we now consider that the base of the LVL has some dip. In this case, the deviation from the vertical raypath assumption is not just controlled by the velocity ratio but also by the dip of the LVL. Even though PS-raypaths show steeper angles on the receiver side leading to a near-vertical condition after conversion, when the base of the LVL is dipping the rays are deviated from this condition in their propagation through the LVL. Figure 1 shows the geometry of this problem.
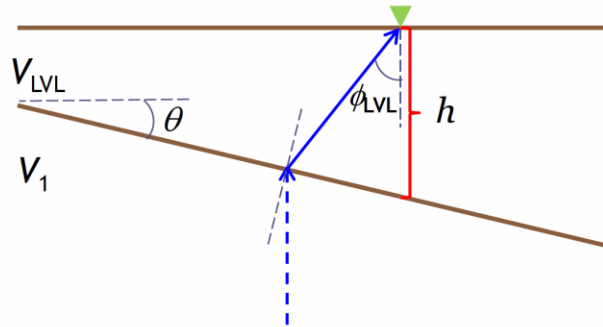
Figure 1: Geometry used for computing raypath-dependent travel times for a dipping LVL. Here, h is the vertical thickness of the LVL at the receiver location, ϕ_{LVL} is the ray-path angle in the LVL, θ is the dip angle at the base of the LVL, V_{LVL} is the velocity of the LVL and V_1 is the velocity of the underlying medium.

The travel time along the solid ray depicted in Figure 1 can be computed using the following expression:

$$t = \frac{h}{v_{LVL}}\frac{\cos(\theta)}{\cos(\phi_{LVL}+\theta)}. \tag{3}$$

where θ is the dip angle of the base of the LVL.

In Figure 2 we can see the combined effect of the dip of the LVL and the variation of the raypath angles on the computation of traveltimes as predicted by equation 3. The zone in which the deviation of the vertical travel times versus deviated travel times is less than 10 ms can be considered as a safe zone since this delay falls into the order of magnitude of the residual statics. However, for dip

angles outside this zone we can expect traveltime increments in the order of tens of milliseconds when the raypath angle changes. Under this condition surface consistency is no longer valid. For a fixed receiver location we will need a travel time correction that may change with the raypath angle. In addition, non-stationarity will arise when the depth of the reflector is considered. This effect is studied in the next section.
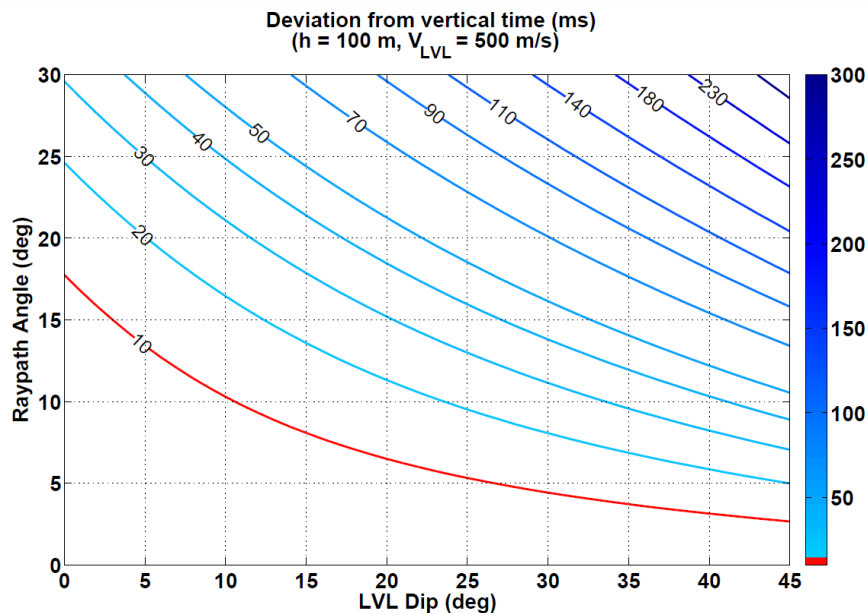

Figure 2: Expected deviation from the vertical ray-path assumption when changes on the dip of the LVL and the transmission ray-path are considered.

Ray Tracing

Figure 3 shows the ray-tracing result for the velocity model at the left. No P-wave velocity contrast was included in the LVL in order to avoid P-wave statics. The colour of each receiver shows the transmission angle of the upgoing rays through the LVL. For the reflector 1, it is possible to identify a change from 0° in the near offsets up to 18° in the far offset. The same change should be observed for a single receiver and several shots. For the deep reflector the range of angles is smaller, with a maximum of 14° at the maximum offset. Since each reflector experienced different transmission angles, the delays suffered by each reflector will be different, even for the same receiver.

In Figure 4 are shown the reflection times for the raytracing done above. Each reflection time is colored by the transmission angle related to each offset. Results show that reflection times with the same transmission angle, i.e. the same static, are not located at the same offset. The black arrows indicate the lateral shift of reflection times that should have traveled the same distance through the LVL and that should receive the same static correction. Furthermore, for the same offset, i.e. the same receiver location, reflections coming from different depths show different transmission angles, hence they should receive different static corrections, implying non-stationary statics. In conclusion, under these conditions non-surface consistency must be taken into account for computing S-wave statics.
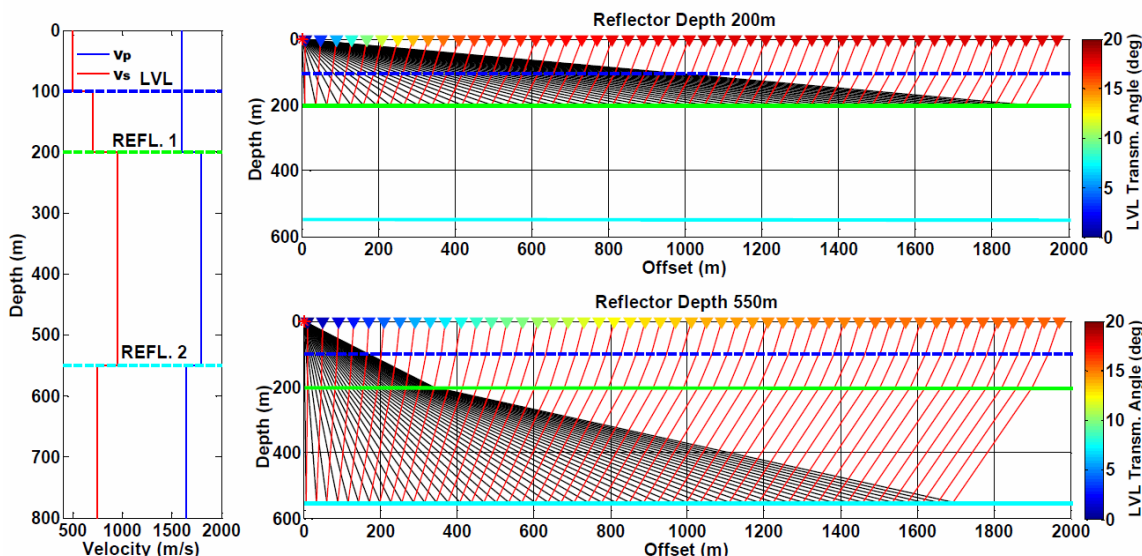
Figure 3: (left) Velocity model used for ray-tracing. (top) PS-raytracing for the shallow reflector. (bottom) PS-raytracing for the deep reflector. The colour of each receiver represent the transmission angle through the LVL.
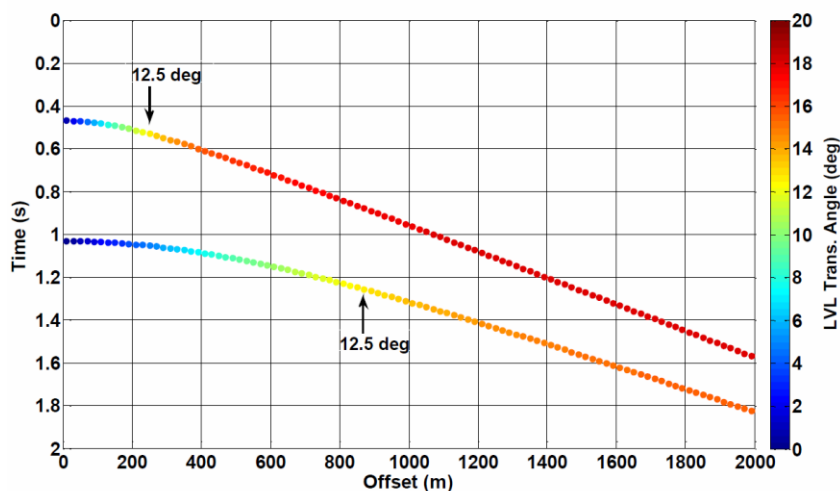

Figure 4: Angles of transmission for each reflector time given by the raytracing. Black arrows indicate how the 12.5⁰ transmission angle is located at different offsets depending on the reflector.

In order to address the problem of a dipping LVL and validate the predicted traveltimes given by equation 3, 2D ray-tracing over a gridded model was performed. A low velocity layer with a dip of 45° and velocity of 500 m/s was used for the raytracing (Figure 5, left). The vertical thickness under the receiver location was set at 50 m. Figure 5 (right) shows a very good match between the travel times given by the analytic formula and those given by the raytracing. The raytracing times display some numerical noise due to the resolution of the gridded model used (1 m).

This match confirms that equation 3 may be used as the engine for the forward modelling of raypath-dependent traveltimes. Moreover, matching these traveltimes with the numerical results for a 2D gridded model also leads us to considerer a tomographic inversion as a plausible tool for building a velocity model for the near surface using raypath-dependent statics.

Stationarity in the radial trace domain

Since the radial-trace (R-T) transform has the effect of approximately simulating seismic data recorded along straight raypaths (Henley, 2000), synthetic PS data was computed, NMO-correcteded, gathered by receiver location and transformed to the R-T domain to study the consistency of the statics with the raypath angle.
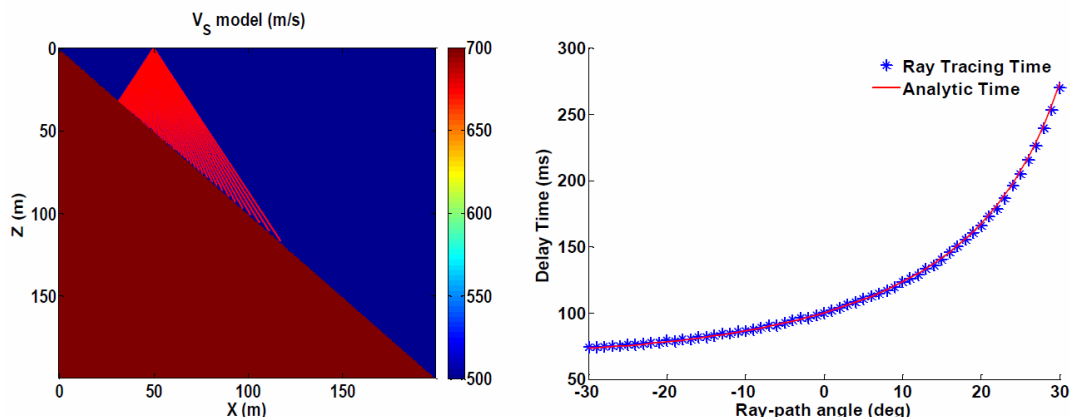

Figure 5: (left) 2D velocity model with a LVL dipping at 45° used for raytracing. In red we can see rays ranging from -30° to 30° respect to the receiver location. (right) Analytic and raytracing travel times for a 45° dipping LVL.

Figure 6 shows the velocity models used for computing the synthetic data. Note that no LVL was included in the P-wave velocity model to avoid shot statics. However, in the S-wave velocity model a deformed LVL was included with a velocity of 500 m/s and thickness ranging from 20m to 100m. Both layers were set as flat to focus our attention on deformations produced by the LVL.
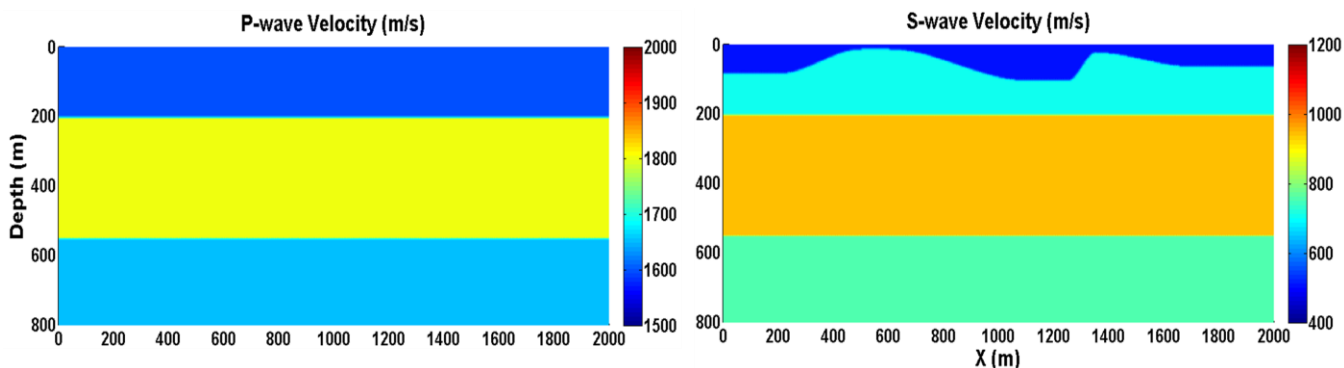

Figure 6. P- and S-wave velocity models used for computing PS synthetic data using 2D finite difference modelling.

Figure 7 shows a zoom on the reflection times for each reflector at a fixed receiver location. By comparing reflection times we can note that there is a time difference between reflection times recorded at positive and negative offset. Since reflectors are known to be flat the source of this difference must be the structure of the near surface. Moreover, the time difference for the shallow reflector has an extra delay of 13 ms compared to the deep reflector. This is a clear evidence of the non-stationarity of the statics. If the proper shift for aligning the amplitudes of the shallow reflector is applied, the deep reflector will be still missaligned by 13 ms, making it impossible to get a good stack for both reflectors simultaneously.
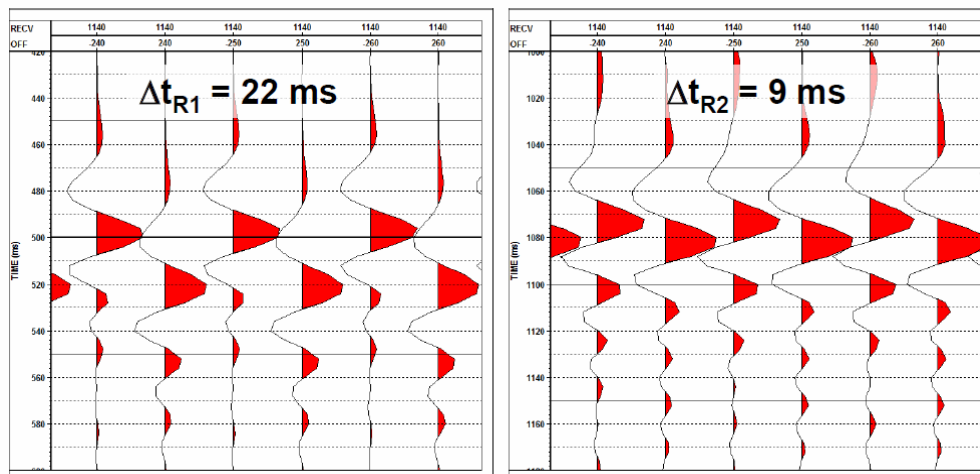
Figure 7. Zoom window around the shallow (left) and deep (right) reflectors in the X-T domain. Traces are sorted by offset value.

The same analysis was performed on the R-T domain traces, for the same receiver location as before. The results are shown in Figure 8. By comparing traces with the same radial-trace value we can note that the time difference between amplitudes at positive and negative R-T values amounts to just 2ms between both reflectors. Although there is still a residual static, the R-T transform was able to move the static problem to a domain where it shows an approximatly stationary behaviour.
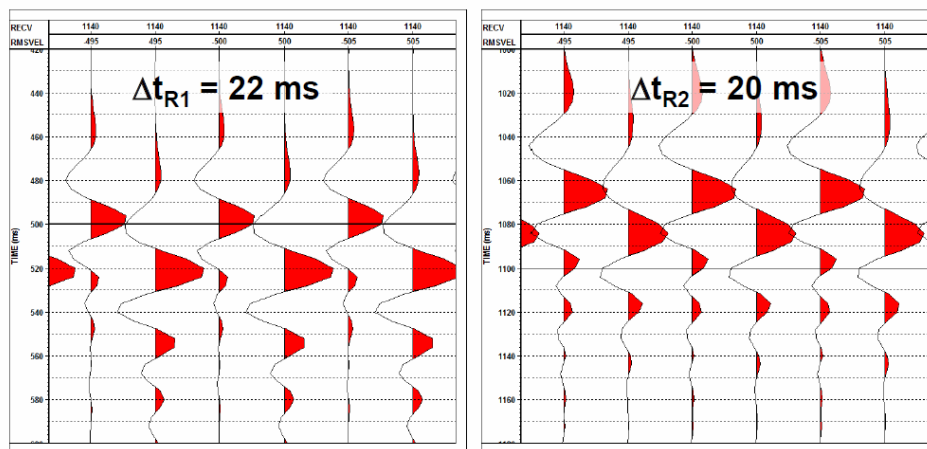

Figure 8. Zoom window around the shallow (left) and deep (right) reflectors in the R-T domain. Traces are sorted by radial-trace value.

Figure 9 shows a comparisson between a stacked section after surface consistent (left) and raypath consistent static corrections (right). For the surface consistent correction, vertical traveltimes were computed at each receiver location and then removed from the traces. For the deep reflector we can note that although there is still some deformation in the geometry of the reflector, it has better coherency and is slightly flatter than the shallow reflector. This is a result of closer near-to-vertical raypaths for the deep reflector compared to the shallow reflector. For the latter we can see that the geometry of the reflector is still affected in an important degree by the near-surface geometry.

In Figure 9 (right) we can note how removing the statics in the R-T domain effectively solved the statics problem on both reflectors. Flatness and coherency and superior after using a raypath-consistent static solution. This is a result of the ability of the R-T domain to accommodate the non-stationary character of the static problem.
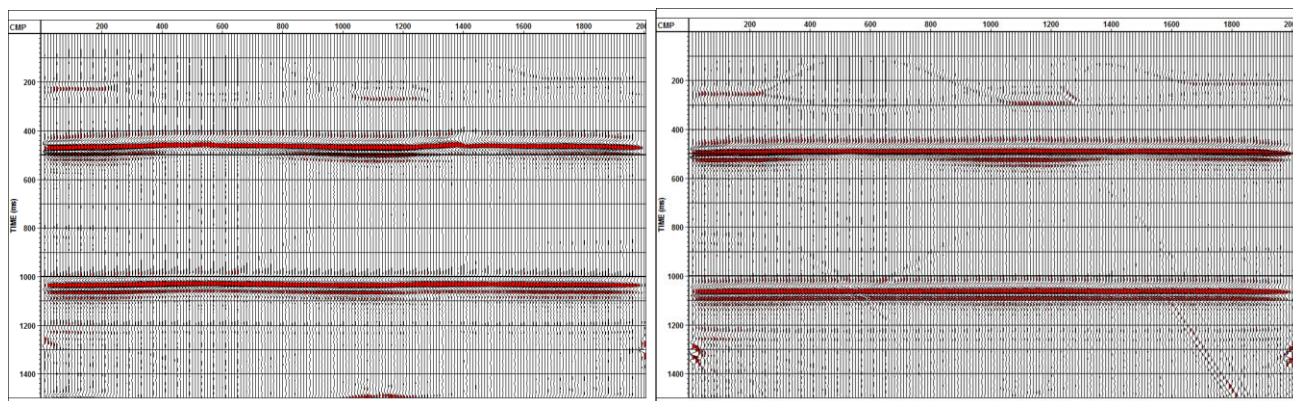

Figure 9. Stacked sections after surface-consistent (left) and raypath-consistent (right) static corrections.

Conclusions

Synthetic data computed using elastic finite difference modelling showed the effects of the LVL structure on the statics. Dips in the LVL can deviate the ray-paths and change the magnitude of the static depending on the direction of propagation. This also leads to a non-stationary effect. Wavefronts coming from different reflectors can arrive at the same point, at the base of the LVL, with dissimilar angles, leading to different statics correction.

The R-T transform was able to move the static problem to a domain in which statics seem to be stationary. This was done by gathering the same trace reflections that should have traveled with approximately the same rayparameter value. Since the R-T transform used here assumes straight ray-paths there are still residual statics that need to be fixed. The Snell ray transform looks to be a very good candidate for improving the effectiveness of the R-T transform for solving non-stationary statics.

As suggested by Equation 6, it is in principle possible to characterize the LVL given a set of ray-path dependent statics for a fixed location. We view the solution of this inverse problem as a key step towards achieving the ultimate goal of computing a S-wave velocity model for the near surface.

Acknowledgements

References

Cox, M., 1999, Static corrections for seismic reflection surveys: Society of Exploration Geophysicists.
Henley, D., 2000, More radial trace domain applications: CREWES Research Report, **12**, 21.1–21.14.
Henley, D., 2012, Interferometric application of static corrections: Geophysics, **77**, No. 1, Q1–Q13.